Effect of electron spectral diffusion on static dynamic nuclear polarization at 7 Tesla

Alisa Leavesley, Daphna Shimon, Ting Ann Siaw, Akiva Feintuch, Daniella Goldfarb, Shimon Vega, and Ilia Kaminker, Songi Han

Electronic Supplemental Information:

ELDOR spectra are the reduction of the echo intensity as a function of excitation frequency (ν_{excite}) and provide insight into the electron depolarization profile when irradiated with microwaves (MW). Experimental ELDOR spectra of the 10 mM and 40 mM 4-amino TEMPO (4AT) samples in a d_8-gylcerol/D_2O/H_2O glass at 4 K and 7 T are shown in figure S1 at a variety of detection frequencies (ν_{detect}) that span the entire nitroxide EPR line. Each ELDOR spectrum has a sharp strong peak that corresponds to ν_{detect}=ν_{excite}, which is the allowed transition. Additional side peaks can be identified as the forbidden single quantum transitions due to hyperfine interactions with the surrounding nuclei (these are the sharp but weaker peaks generally offset by ≤ 50 MHz for ^{14}N and 300 MHz for ^{1}H) as discussed by Florent et al.[1] In the 10 mM 4AT sample, the ^{1}H forbidden transition is seen to shift as ν_{detect} is shifted and that little to no depolarization is seen at the center of the EPR line, which we have attributed to electron spectral diffusion (eSD) in higher concentration samples such as 40 mM 4AT (see main text). It is interesting to note that the large depolarization we have assigned as eSD in the 40 mM 4AT sample is observed independently of ν_{detect}. The central depolarization that is independent of ν_{detect} is a hallmark of significant eSD effects in a system.

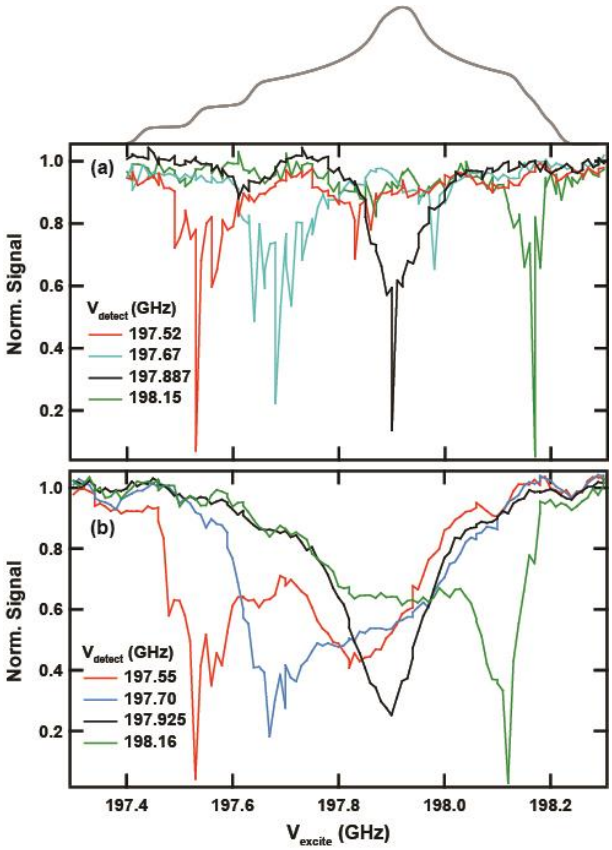

Figure S1. *ELDOR spectra of 10 mM (a) and 40 mM (b) 4-amino TEMPO in a d_8-gylcerol/D_2O/H_2O glass at 4 K and 7 T for varying ν_{detect} as defined inside the figure. The nitroxide EPR line is above the ELDOR spectra as a reference of the relative electron populations. Experimental parameters are t_{sat} = 100 ms, repetition time = 400 ms, t_p = 500 ns, t_d = 10 µs, and τ = 500 ns.*

Simulated ELDOR curves for the four different concentrations used in this study: 1.7, 10, 20, and 40 mM, are an intermediate result in calculating simulated DNP profiles, where each ELDOR curves represents the electron depolarization spectrum at a single detection frequency, which when compiled across the entire EPR line are used to extract the depolarization profile for a single excitation frequency (Fig. S2). The ELDOR curves are presented as a function of the MW excitation frequency; therefore, three different detection frequencies are shown to clearly observe the electron spectral diffusion effect across the EPR line. At the lowest concentration (1.7 mM), where the SE-DNP mechanism is the dominant mechanism, the hyperfine interactions between the electron and ^{1}H can be observed as peaks that are offset by the ^{1}H Zeeman frequency – here 300 MHz. As the radical concentration is increased, the electrons become ever closer, such that electron spectral diffusion (eSD) is possible. eSD induces the broadening of the peak where the excitation and detection frequencies are the same as well as the growth of the broad peak at the center of the nitroxide EPR spectrum due to the high electron population.

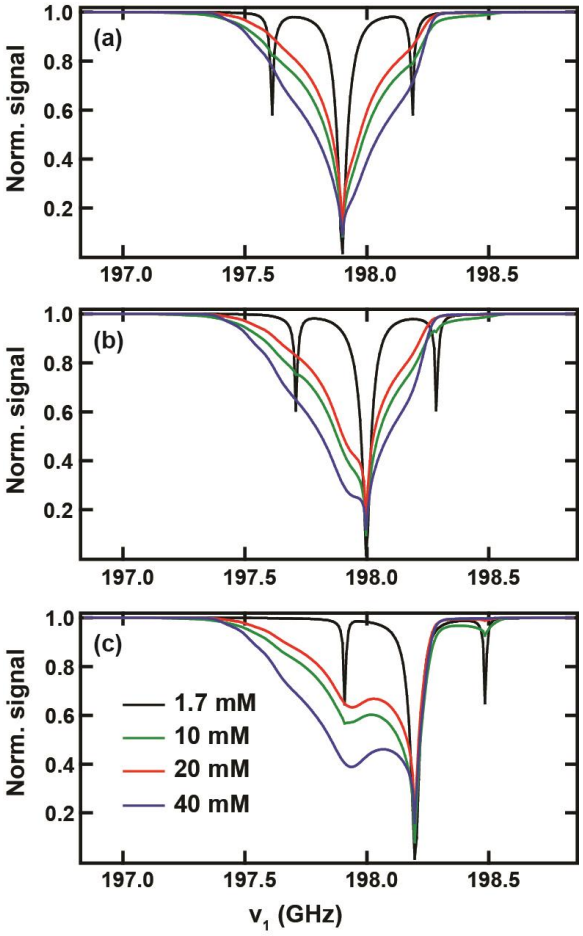

Figure S2. *Simulated ELDOR curves for 4-amino TEMPO at 4K at multiple radical concentrations, as defined inside the figure. Three detection frequencies are shown, where* ν_{detect} *= 197.9 GHz (a),* ν_{detect} *= 198 GHz (b), and* ν_{detect} *= 198.2 GHz (c). The parameters used in the simulations are given in Table 1 of the main text.*

To quantify the sensitivity of the simulations to variations in the fitting parameters, an overall quality parameter, σ_{DNP}, that equals to the sum of the squares of the differences between the values of the experimental enhancements and the simulated ones is used to determine the sensitivity of the simulations to variations in T_{2e}

and Λ^{eSD}.[2] From these contour plots we can see that variations in T_{2e} cause little to no change in σ_{DNP}, unless T_{2e} is small for all four concentrations used in this study (Fig. S3). As the concentration is increased the sensitivity of σ_{DNP} to Λ^{eSD} is reduced. The yellow circles mark the T_{2e} and Λ^{eSD} values used to simulate the ELDOR spectra above and given in Table 1 of the main text.

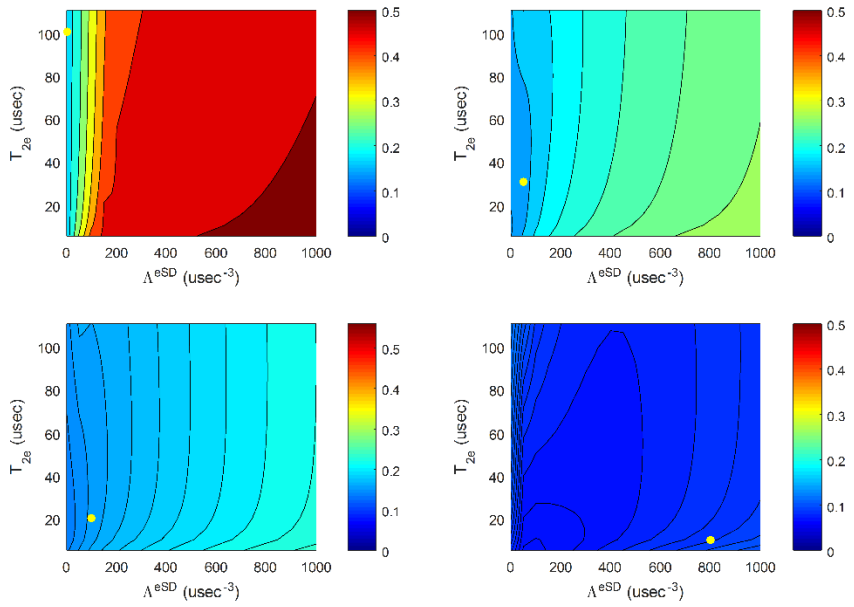

Figure S3. *Contour plots of σ_{DNP} as a function of T_{2e} and Λ^{eSD} for 1.7, 10, 20, and 40 mM. The yellow circles mark the T_{2e} and Λ^{eSD} values given in Table 1 of the main text.*

The parameter describing the width of the DNP spectrum, Δw_{DNP}, is used as a general descriptor of the overall breadth of the DNP spectra. However, to make sure that the Δw_{DNP} is an accurate representation of the DNP profiles overall lineshape, specifically its breadth, the span of experimental and simulated DNP spectra at relative signal intensities were plotted as a function of radical concentration for 12.5, 25, 50, and 75% of the signal intensity, where the span from positive to negative was considered (Fig. S4b). A pictorial representation of these spans at different signal intensities is shown in Fig. S4a, while the actual spans for simulated and experimental DNP profiles at the different signal intensities as a function of radical concentration are shown in Fig S4b. As a function of concentration, all of the different signal intensities, except for 100% (Δ_{DNP}), show similar results, suggesting the use of Δw_{DNP} is a valid descriptor of the overall DNP spectral lineshape breadth.

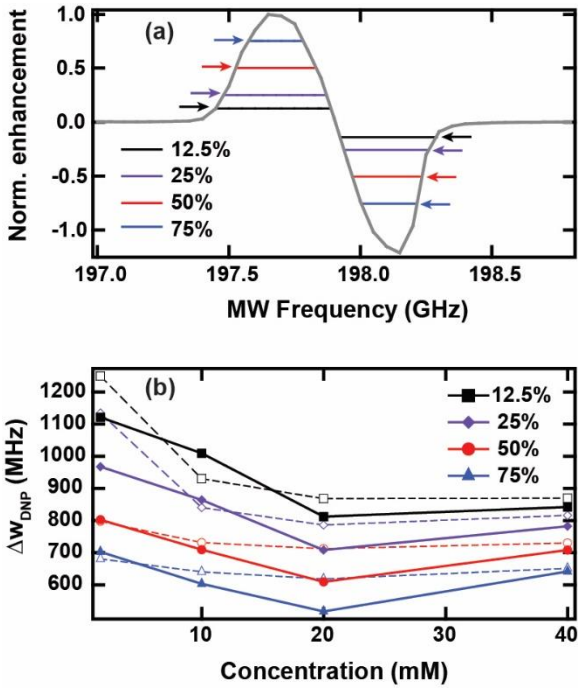

Figure S4. *The span of the spectrum at 12.5%, 25%, 50%, and 75% is depicted in (a). Normalized experimental and simulated DNP profile widths according to the span of the profile at 12.5%, 25%, 50%, and 75% of the normalized NMR signal intensity were plotted versus radical concentration. Simulated spectra are depicted with dashed lines and experimental data is represented with solid lines, where the lines are to guide the eye. Specifically,* Δw_{DNP} *is when the signal intensity is 50%.*

Simulated ELDOR curves were used to make electron depolarization profiles for a single excitation frequency, which were then used to calculate the temperature dependent simulated DNP (Fig. S5). Each ELDOR curve represents the electron depolarization spectrum as function of the excitation frequency for a single detection frequency. Compiled ELDOR curves can then be used to extract the depolarization profile for the excitation frequencies that are used for the calculation of the DNP spectrum. Three representative ELDOR curves are shown for each temperature in figure S5. The normalized simulated DNP spectra are in good qualitative agreement with the experimental temperature dependent data. The negative enhancement peak of the normalized simulated ELDOR spectra are consistently slightly less than one. For the experimental DNP spectra there is a slight reduction of the negative enhancement peak in the DNP spectra with increasing temperature. The span of the temperature dependent DNP spectra at 12.5, 25, 50, and 75% of the signal intensity is plotted as a function of temperature to confirm the use of Δw_{DNP} as an accurate representation of the overall DNP breadth when considering temperature dependence (fig. S6). This comparison shows that the use of only the 50% of the signal intensity to represent Δw_{DNP} is an accurate representation of the DNP spectral lineshape.

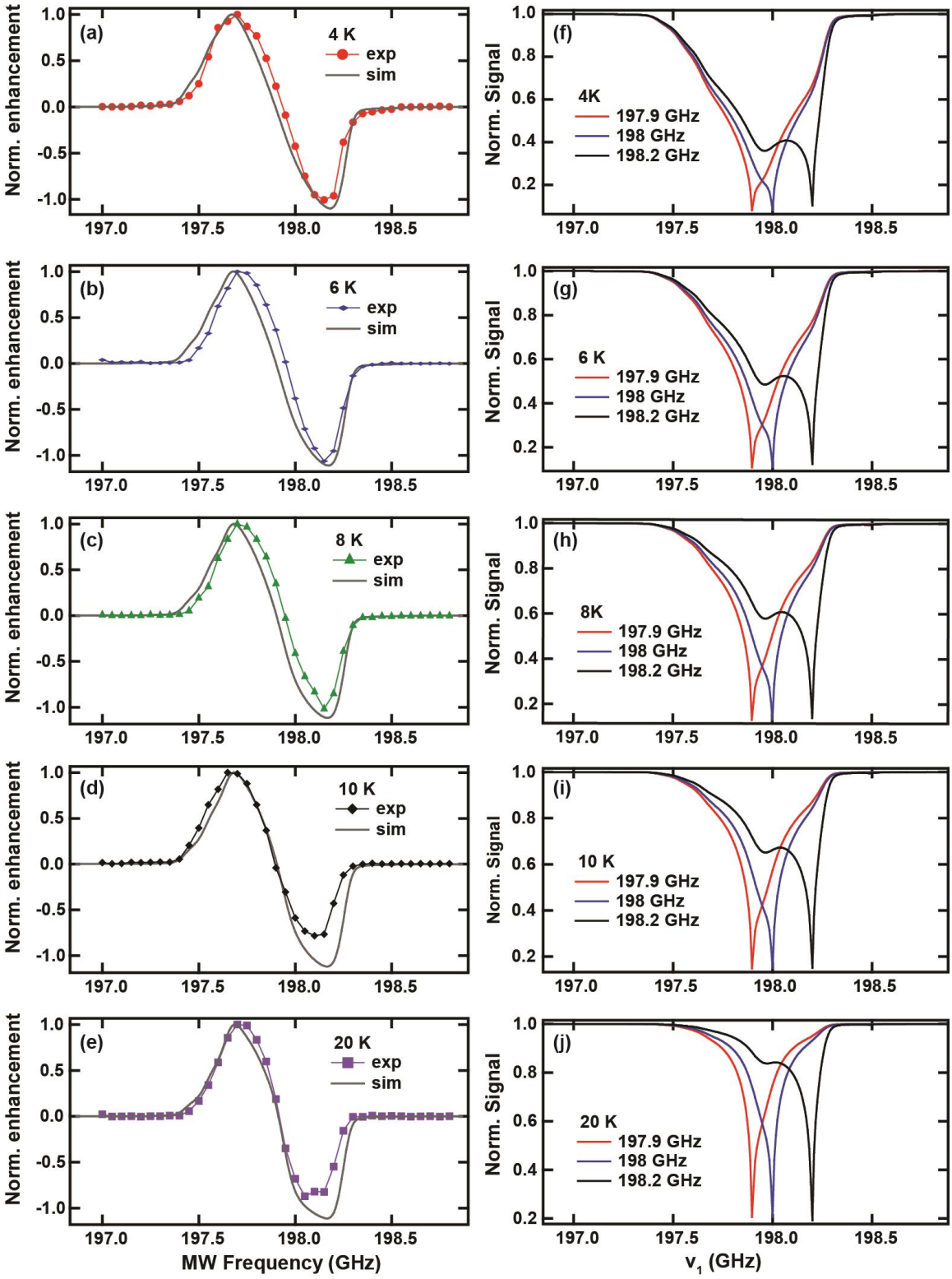

Figure S5. *Normalized experimental and simulated DNP profiles for 40 mM 4-amino TEMPO were compared across multiple temperatures (a-e). The temperatures and designation of experimental or simulation are defined inside the figures. (f-j) Corresponding simulated ELDOR curves for the different temperatures 4K, 6K, 8K, 10K, and 20K are shown at detection frequencies* ν_{detect} *= 197.9 GHz (red),* ν_{detect} *= 198 GHz (blue),* ν_{detect} *= 198.2 GHz (black). The parameters used for the simulations are given in Table 2 of the main text.*

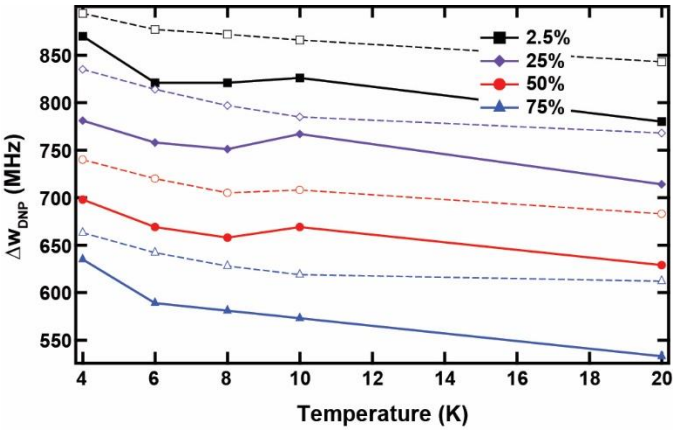

Figure S6. *Normalized experimental and simulated DNP profile widths, Δw_{DNP} were plotted versus temperature, where the width is determined by the breadth of the profile when the signal is at 12.5%, 25%, 50%, and 75% of the normalized DNP profile. Specifically, Δw_{DNP} is when the signal intensity is 50%.*

When considering the power dependence of the 40 mM 4AT sample at 4 K, simulations where only ν_1 are varied need to be considered (Fig. S7). The simulated ELDOR curves have a minimal broadening effect with increasing ν_1. This is also reflected in the simulated DNP spectra, where the simulated DNP spectra have almost no discernible difference at low ν_1. It is interesting to note that at high enough powers, the simulated spectra result in DNP signal intensity that spans more than 1.8 GHz. To confirm that the parameter Δw_{DNP} is an accurate representation of the DNP spectral lineshape, the span of the DNP signal intensity at 12.5, 25, 50, and 75% were shown for the experimental and simulated spectra in figure S8. The agreement of 12.5, 25, 50 and 75% for concentration, temperature, and MW irradiation strength dependent data suggests that the use of Δw_{DNP} is an accurate overall representation of the DNP spectral linewidth.

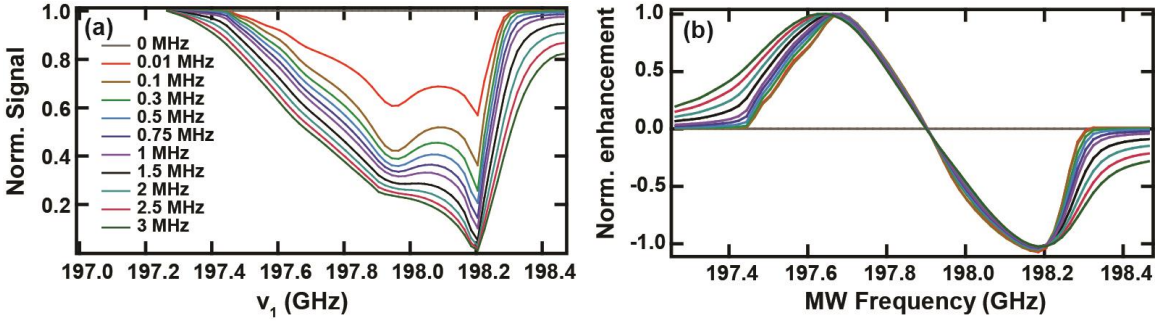

Figure S7. *Simulated ELDOR (a) and DNP profiles (b) of 40 mM 4-amino TEMPO at 4K for varying MW irradiation strengths as defined inside the figure. The simulation assumes a constant Λ^{eSD} of 800 μs^3 for each irradiation strength, ν_1, and the ELDOR curves have a detection frequency of ν_{detect} = 198.2 GHz. The parameters used for the simulations are given in Table 1 of the main text.*

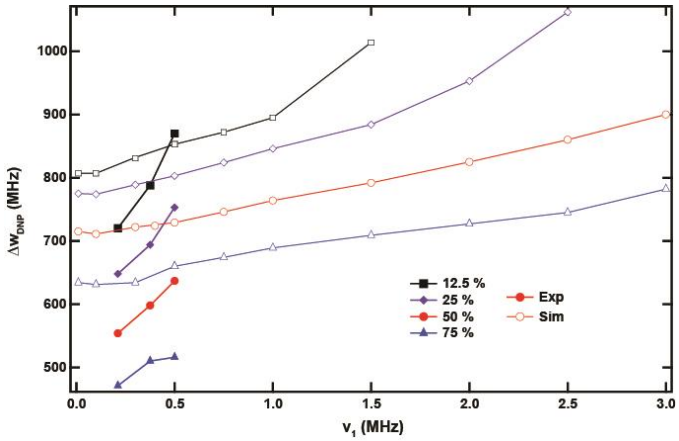

Figure S8. *Normalized experimental (solid symbols) and simulated with constant A^{eSD} (solid line – open symbols) DNP profile widths (Δw_{DNP}) were plotted versus temperature, where the width is determined by the breadth of the profile when the signal is at 12.5%, 25%, 50%, and 75% of the normalized DNP profile. Specifically, Δw_{DNP} is for when the signal intensity is 50%.*

The observed experimental broadening of Δw_{DNP} with increasing ν_1 is a consistent observation across multiple days, sample compositions, and freezing conditions. For glycerol/water samples, similar increases in Δw_{DNP} were observed independently of the glycerol concentration and the freezing condition (fig S9). The two freezing conditions were rapid freezing where the samples were frozen at a rate of 10 K/min from room temperature to 4 K, while during annealed freezing the samples were frozen at a rate of 1 K/min and underwent an hour long isotherm 10 K above the glass transitions temperature (T_g). The consistent change in Δw_{DNP} with increasing ν_1 confirms that this observation is real and not a result of experimental error.

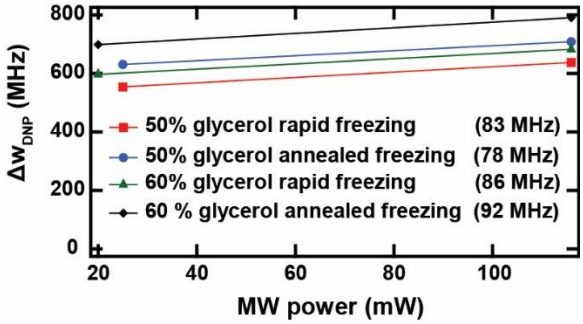

Figure S9. *Normalized experimental Δw_{DNP} for high and low powers of MW irradiation for different sample compositions and freezing conditions, where rapid freezing denotes freezing at 10 K/min, while annealed freezing denotes freezing at 1K/min with an hour isotherm at 10 K above the T_g. The numbers in parentheses are the difference between the Δw_{DNP} values at high and low power for that sample.*

The power dependence of DNP enhancement for a 40 mM 4AT sample can be best observed in a power curve, where the DNP enhancement is plotted as a function of the MW irradiation strength, ν_1. The simulated and experimental power curves are plotted in figure S10. The simulated enhancements when assuming only ν_1 changes are plotted until the oversaturation effect is observed; the threshold ν_1 for oversaturation in this simulation method is ~2.5 W (1.5 MHz), which is experimentally impossible for our instrument's current capabilities.

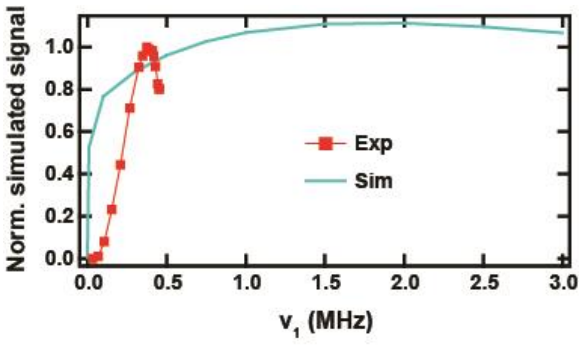

figure S10. *Experimental (red – symbols) and simulated power curvs with constant Λ^{eSD} (aqua –solid line). The maximum experimentally relevant MW irradiation strength for our instrumentation is 0.5 MHz.*

References

1 M. Florent, I. Kaminker, V. Nagarajan and D. Goldfarb, *J. Magn. Reson.*, 2011, **210**, 192–199.

2 I. Kaminker, D. Shimon, Y. Hovav, A. Feintuch and S. Vega, *Phys. Chem. Chem. Phys.*, 2016, **18**, 11017–11041.